Dissipative multistate systems in the scaling limit

Manfred Winterstetter
II. Institute of Theoretical Physics, University of Stuttgart, D-70550 Stuttgart, Germany
(Received 9 February 1999)

The dynamics of dissipative multistate systems is studied using integral equations that are derived within the framework of the path integral-formulation of quantum mechanics. As an illustrative example we study a 5-state system coupled to a harmonic reservoir with an Ohmic spectral density with a high cutoff frequency. The dominant exchange mechanism determining the dynamics as well as the range of validity of different approximations to the influence functional are investigated. Besides depending on temperature and the strength of the system-bath coupling, both the exchange mechanism and the accuracy of different approximations to the influence functional depend on the state in which the system is initially prepared. [S1063-651X(99)07307-9]

PACS number(s): 05.30.−d

I. INTRODUCTION

Quantum Brownian motion is an archetype system for many problems in physics and chemistry. It describes the dynamics of a particle in a multiwell potential that is coupled to an environment [1]. In the deep quantum regime, the dynamics of such a particle may be modeled by a *M*-state system, where a single localized state corresponds to each minimum of the potential [2]. The case where the system can be confined to just two states, the familiar spin-boson system, has found widespread application to various biological, chemical, and physical systems (see [2], and references therein). Dissipation is induced by a bilinear coupling to a heat bath, which is commonly represented by a set of harmonic oscillators. Another familiar picture is the tight-binding representation of a quantum particle in a periodic potential under the influence of a bath. If there is only a single localized state in each well, the system is then equivalent to an infinite one-dimensional lattice. Within the path-integral formulation of quantum mechanics [2–5], it is possible to eliminate a harmonic reservoir. The effect of the environment is then described by a time-nonlocal influence functional [4,2,6].

Many transport phenomena in condensed matter physics can be modeled by quantum Brownian motion in a cosine potential [7]. The case of frequency-independent damping applies to the electron-hole drag of charged particles in metals and quasiparticle tunneling in Josephson junctions [7,8]. Charge transport through impurities in quantum wires [9] as well as edge currents in fractional quantum Hall devices [10] are further applications of the model. In this approach, collective excitations of correlated electrons constitute the reservoir of the quantum Brownian particle. The model has also been applied to study the current-voltage characteristic in a small Josephson junction [7,8,11], and to study the quantum diffusion of charged interstitials in metals [12]. In principle, the number of localized states in an extended periodic potential is infinite. In numerical simulations the lattice can only be represented by a limited number of sites and finite-size effects must be investigated carefully. We study the time evolution of the reduced density matrix of the *M*-state system. In the results discussed in this work, we choose a 5-state system, a choice that is somehow arbitrary. If one aims to calculate transport properties such as the nonlinear mobility or diffusion coefficients, the initial state on the infinite grid can be chosen arbitrary. If, on the contrary, one wants to study the transport along a chain, the initial sites must be chosen as the edge states.

Recently, a description of the reduced dynamics in terms of integral equations termed interacting blip chain approximation (IBCA) was derived for the dissipative two-state system [13]. This approach is generalized to *M*-state systems in the present paper. In principle, the range of the memory in the influence functional is unlimited, and thus the numerical treatment is tedious. Approaches based on the Trotter split up [14–18], which take into account all or at least long-range interactions entering the influence functional, are computationally demanding and suffer from the ubiquitous sign problem [19–21]. If the coupling to the environmental modes is weak and/or the temperature is high, the Markov approximation can be applied, bringing about significant simplifications [2,22–25]. Although substantial progress has been made on the analytical side [26–29], numerical calculations are inevitable for low temperatures and intermediate coupling strength. However, if the spectral density of the bath is Ohmic with a high cutoff frequency, the correlations between different segments of an individual path decay rapidly and consequently considering only local contributions or next-neighbor interactions yields a reliable description of the dynamics in a wide range of the parameter space. In this paper, we present results for systems in which the typical bath frequency is by far the highest frequency entering the model. This parameter regime is often denoted as *scaling limit*. Our algorithm is iterative in time and the scaling with the number of discretization points is drastically reduced in comparison with a full treatment of the dynamics. For a *M*-state system and *N* elementary intervals the number of paths in the Trotter path integral is M^{2N}, whereas in the IBCA with next-neighbor interactions the number of configurations is only $[(M+1)M/2]^2\times[(N+1)N]/2$. In principle, the IBCA can be improved to any desired accuracy but becomes practically untractable.

The paper is organized the following way. In Sec. II the model is presented. In Sec. III, the dynamical quantities and the formally exact solution are given. The dynamical equations resulting from the IBCA are derived in Sec. IV and

applications are discussed in Sec. V. Finally, in Sec. VI, conclusions are drawn and an outlook is given.

II. THE DISSIPATIVE *M*-STATE MODEL

We consider a *M*-state system coupled to a bosonic bath. The states $\{|\varphi_j\rangle\}_{j=1,\ldots,M}$ of the tight-binding system with energies $\{e_j\}_{j=1,\ldots,M}$ are coupled by next-neighbor intersite coupling matrix elements. We assume that all next-neighbor coupling matrix elements are equal. Dissipation is induced by the coupling to an Ohmic bath. The Hamiltonian reads

$$H=H_{\mathrm{TB}}+H_{\mathrm{B}}+H_{\mathrm{int}}. \tag{1}$$

Here, H_{TB} is the Hamiltonian of the bare tight-binding system given by

$$H_{\mathrm{TB}}=\frac{1}{2}\begin{pmatrix} e_1 & 0 & 0 & 0 & \ldots \\ 0 & e_2 & 0 & 0 & \ldots \\ 0 & 0 & e_3 & 0 & \ldots \\ 0 & 0 & 0 & e_4 & \ldots \\ \ldots & \ldots & \ldots & \ldots & \ldots \end{pmatrix} - \frac{\Delta}{2}\begin{pmatrix} 0 & 1 & 0 & 0 & \ldots \\ 1 & 0 & 1 & 0 & \ldots \\ 0 & 1 & 0 & 1 & \ldots \\ 0 & 0 & 1 & 0 & \ldots \\ \ldots & \ldots & \ldots & \ldots & \ldots \end{pmatrix}, \tag{2}$$

and the bath and the system-bath interaction are taken into account by

$$H_{\mathrm{B}}=\sum_{\alpha}\left(\frac{p_\alpha^2}{2m_\alpha}+\frac{m_\alpha\omega_\alpha^2}{2}x_\alpha^2\right)\hat{I}, \tag{3}$$

$$H_{\mathrm{Int}}=\sum_{\alpha}\left(-c_\alpha x_\alpha\hat{Q}+\frac{c_\alpha^2}{2m_\alpha\omega_\alpha^2}\hat{Q}^2\right). \tag{4}$$

$\hat{I}$ is the identity in the Hilbert space of the tight-binding system. The first term in H_{int} describes the bilinear system-bath coupling, and the second term represents a counterterm, which renders the system translationally invariant. The position operator $\hat{Q}$ of the tight-binding particle is given by

$$\hat{Q}=q_0\,\mathrm{diag}(1,2,3,\ldots)+\overline{q}\hat{I}, \tag{5}$$

where q_0 measures the spacing of the tight-binding lattice. The shift $\overline{q}$ is a measure of the polarization of the bath. The states of the *M*-level system correspond to *M* localized states in a potential energy function. The reduction of the system dynamics to such a *M*-level system is justified, if the other discrete states are energetically well separated from these lowest *M* states.

The influence of the bosonic bath on the tight-binding system is captured by the spectral density function

$$J(\omega)=\frac{\pi}{2}\sum_{\alpha}\frac{c_\alpha^2}{m_\alpha\omega_\alpha}\delta(\omega-\omega_\alpha). \tag{6}$$

In the numerical calculations presented in this paper, we assume a continuous spectral density of Ohmic form,

$$J(\omega)=(2\pi\alpha\omega/q_0^2)\exp\left(-\frac{\omega}{\omega_c}\right). \tag{7}$$

In our notation α is the dimensionless Kondo parameter, that describes the strength of the bilinear system-bath coupling, and ω_c is a high-frequency cutoff setting the typical time scale of the dynamics of the bath. Our approach is, however, not restricted to a certain form of the spectral density. In principle any number of discrete modes as well as any continuous spectral density can be treated.

III. DYNAMICAL QUANTITIES AND FORMALLY EXACT SOLUTION

We are interested in the dynamics of the reduced density matrix,

$$\langle\rho_{kl}(t)\rangle_\beta=tr_{\mathrm{bath}}\langle\varphi_{in}|\langle\exp(iHt)/\hbar|\varphi_k\rangle \times\langle\varphi_l|\exp(-iHt)\rangle_\beta|\varphi_{\mathrm{in}}\rangle, \tag{8}$$

where at time $t=0$ the system is prepared in a factorizing initial state $\rho_{kl}(0)=\delta_{k,\mathrm{in}}\delta_{l,\mathrm{in}}\langle\rho_B\rangle_\beta$ with the bath in thermal equilibrium. $\langle\rangle_\beta$ denotes the thermal average with respect to the bath, $\beta=1/k_BT$ is the inverse temperature, and the $|\varphi_j\rangle$ are the states of the tight-binding system. Equation (8) can be expressed in terms of a double path integral:

$$\langle\rho_{kl}(t)\rangle_\beta=\int\mathcal{D}q\int\mathcal{D}q'\,\mathcal{A}[q]\mathcal{B}[q]\mathcal{A}^*[q']\mathcal{B}^*[q'] \times\exp\{-\Phi_{\mathrm{FV}}[q,q']\}. \tag{9}$$

Here, the quantity $\mathcal{A}[q]$ is the probability amplitude of the tight-binding system associated with the path $q(t)$ in the absence of biasing and fluctuating forces. The deterministic biasing forces are encapsulated in the factor

$$\mathcal{B}[q]=\exp\left\{-i\int_0^t dt'\,\epsilon[q(t')]\right\}. \tag{10}$$

The influence function $\Phi_{\mathrm{FV}}[q,q']$ captures the influences of the fluctuating force $\zeta(t)$. For Gaussian statistics [2],

$$\Phi_{\mathrm{FV}}[q,q']=\int_0^t dt'\int_0^{t'}dt''[q(t')-q'(t')] \times[\langle\zeta(t')\zeta(t'')\rangle_\beta q(t'') -\langle\zeta(t')\zeta(t'')\rangle_\beta q'(t'')].$$

$\int\mathcal{D}q$ in Eq. (9) symbolically denotes summation in the configuration space over all paths with fixed boundaries. As the paths are piecewise constant, the influence function Φ is conveniently expressed in terms of the second integral $Q(t'-t'')$ of the force correlation function $\langle\zeta(t')\zeta(t'')\rangle$. We now introduce the variables [2]

$$\eta(t)=(q(t)+q'(t))/2, \tag{11}$$

$$\xi(t)=(q(t)-q'(t))/2. \tag{12}$$

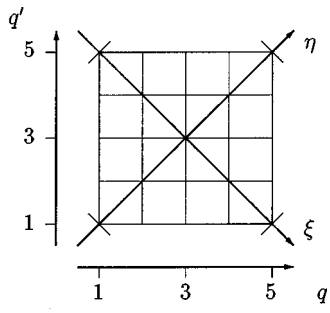

FIG. 1. The quasiclassical coordinate $\eta=(q+q')/2$ and the quantum fluctuations $\xi=(q-q')/2$ are depicted schematically for the reduced density matrix of a 5-state system.

The quasiclassical coordinate $\eta(t)$ describes propagation of the center of mass of the tight binding particle while the so-called quantum fluctuations $\xi(t)$ reflect excursions away from the diagonal of the reduced density matrix. The coordinates are illustrated in Fig. 1 for a 5-state system.

In analogy to Eq. (9), the exact dynamics of the elements of the reduced density matrix is given by

$$\langle\tilde{\rho}_{\eta,\xi}(t)\rangle_\beta=\int\mathcal{D}\xi\exp\{-\mathrm{Re}\,\tilde{\Phi}_{\mathrm{FV}}[\xi]\}\times\int\mathcal{D}_\xi\,\eta\tilde{\mathcal{A}}[\xi,\eta]\tilde{\mathcal{B}}[\xi,\eta]\exp\{-\mathrm{Im}\tilde{\Phi}_{\mathrm{FV}}[\xi,\eta]\},\tag{13}$$

in terms of the coordinates ξ and η. In this representation, we exploit the fact that the real part of the influence function depends on the quantum fluctuations only. Thus the symbolic summation in configuration space can be carried out in two steps. $\mathcal{D}\xi$ denotes summation over all possible configurations of the quantum fluctuations and $\mathcal{D}_\xi\eta$ symbolizes the summation over the manifold of different quasiclassical configurations corresponding to the same quantum fluctuation. Equations (13) and (9) are connected through the relations,

$$\tilde{\mathcal{A}}[\xi,\eta]=\mathcal{A}[q]\mathcal{A}^*[q'],\quad\tilde{\mathcal{B}}[\xi,\eta]=\mathcal{B}[q]\mathcal{B}^*[q'].\tag{14}$$

The contribution depending on the bias is given by

$$\tilde{\mathcal{B}}[\xi,\eta]=\exp\left[-i\int_0^t dt'\,\varepsilon_{\eta_r,\xi_r}(t')\right],$$

$$\varepsilon_{\eta_r,\xi_r}(t)=\epsilon[\eta(t)+\xi(t)]-\epsilon[\eta(t)-\xi(t)].\tag{15}$$

If the system undergoes transitions between different states at the $N-1$ intermediate times t_j within the interval $[t_0,t_N]$, the values of the functions $\eta(t)$ and $\xi(t)$ are piecewise constant on the intervals $\tau_j=t_{j+1}-t_j$, $j=0,\ldots,N-1$. Their values are denoted η_j and ξ_j, respectively. Thus, the influence functional reads

$$\tilde{\Phi}_{\mathrm{FV}}[\eta,\xi]=\sum_{r=0}^{N-1}(\xi_r^2\Lambda_{r,r}-i\xi_r\eta_rX_{r,r})+\sum_{r=1}^{N-1}\sum_{s=0}^{r-1}(\xi_r\Lambda_{r,s}\xi_s-i\xi_rX_{r,s}\eta_s).\tag{16}$$

Here, the first term describes the contributions within the intervals τ_j and the second term captures all interactions between different segments of a path. The $\Lambda_{r,s}$ and $X_{r,s}$ are the real and imaginary parts of the interaction of the interval r with the preceding interval s. Upon introducing the notations $Q_{j,k}=Q(t_j-t_k)$ and $Q(\tau)=Q'(\tau)+iQ''(\tau)$, the interactions read

$$\Lambda_{j,j}=Q'_{j+1,j},\tag{17}$$

$$X_{j,j}=Q''_{j+1,j}-\tfrac{1}{2}\,\tau_j\mu,\tag{18}$$

$$\Lambda_{j,k}=Q'_{j+1,k}+Q'_{j,k+1}-Q'_{j+1,k+1}-Q'_{j,k},\tag{19}$$

$$X_{j,k}=Q''_{j+1,k}+Q''_{j,k+1}-Q''_{j+1,k+1}-Q''_{j,k},\tag{20}$$

with

$$\mu=\sum_\alpha\frac{c_\alpha^2}{m_\alpha\omega_\alpha}=\frac{2}{\pi}\int_0^\infty d\omega\,\frac{J(\omega)}{\omega}.\tag{21}$$

The second term in the expression for $X_{j,j}$ is exactly compensating the counterterm in Eq. (4). The twice integrated kernel of the influence function is given by

$$Q(\tau)=\frac{1}{\pi}\int_0^\infty d\omega\,\frac{J(\omega)}{\omega^2}\,\frac{\cosh(\omega/2T)-\cosh(\omega/2T-i\omega\tau)}{\sinh(\omega/2T)}.\tag{22}$$

Note that $Q''(\tau)$ does not depend on temperature and consequently the validity of approximations to the exact $Q''(\tau)$ is not sensitive to the temperature. For the Ohmic spectral density given in Eq. (7), $Q(\tau)$ reads [30]

$$Q'(\tau)=2\alpha\ln\left(\frac{\Gamma^2(\kappa)\sqrt{1+\omega_c^2\tau^2}}{\Gamma(\kappa+iT\tau)\Gamma(\kappa-iT\tau)}\right),$$

$$Q''(\tau)=2\alpha\arctan(\omega_c\tau),\tag{23}$$

where $\Gamma(z)$ is the gamma function, and $\kappa=1+T/\omega_c$. This form holds for arbitrary cutoff frequency ω_c and we have $\mu=4\alpha\omega_c$. In the limit of large ω_c/Δ, the so-called *scaling limit*, Eq. (23) reduces to

$$Q'(\tau)=2\alpha\ln[(\omega_c/\pi T)\sinh(\pi T\tau)],$$

$$Q''(\tau)=\pi\alpha\,\mathrm{sgn}\,(\tau)\ \text{ with }\ Q''(0)=0.\tag{24}$$

The approximation of $Q''(\tau)$ by a step function simplifies the expressions (18) and (20) for the imaginary part of the influence functional,

$$X_{j,j}=\pi\alpha-\tfrac{1}{2}\,\tau_j\mu,\tag{25}$$

$$X_{j,j-1}=-\pi\alpha,$$

$$X_{j,j-r}=0 \qquad \text{for} \quad r\geqslant 2. \tag{26}$$

The influence function now reads

$$\tilde{\Phi}_{\mathrm{FV}}^{\mathrm{Ohmic}}[\eta,\xi]=\sum_{r=0}^{N-1}\xi_r^2 Q''(\tau_r)+\sum_{r=1}^{N-1}\sum_{s=0}^{r-1}(\xi_r\Lambda_{r,s}\xi_s) -i\alpha\pi\sum_{r=1}^{N-1}\xi_r(\eta_r-\eta_{r-1}). \tag{27}$$

If, in addition to a large cutoff ω_c, one assumes weak coupling and high temperatures, $Q'(\tau)$ can be further approximated by a linearized function,

$$Q'(\tau)=2\alpha\ln\left(\frac{\omega_c}{2\pi T}\right)+2\alpha\pi T\tau. \tag{28}$$

Insertion of Eq. (28) into Eq. (16) leads to the influence functional,

$$\tilde{\Phi}_{\mathrm{FV}}^{\mathrm{lin}}[\eta,\xi]=2\alpha\pi T\sum_{r=1}^{N-1}(\xi_r^2\tau_r)-2\alpha\sum_{r=1}^{N-1}\xi_r^2\ln\left(\frac{\omega_c}{2\pi T}\right) -i\alpha\pi\sum_{r=1}^{N-1}\xi_r(\eta_r-\eta_{r-1}). \tag{29}$$

Here, the boundary condition $\xi_0=0$ is taken into account. This linearization corresponds to a Markov approximation in the real part of the kernel of the influence function $\langle\zeta(t')\zeta(t'')\rangle=K\delta(t'-t'')$. For $\alpha=0.1$ and $\beta=1/\Delta$ the accuracy of the various approximations are illustrated in Fig. 2. In the upper graph in Fig. 2, the correct expression for Q' given by Eq. (23) is compared with the high ω_c approximation given by Eq. (24). The differences vanish on a short time scale. In the inset in Fig. 2(a), the exact expression for Q' is compared with the linearized version of the interaction given by Eq. (28). Please note that the time window in the inset is 25 times bigger than the one in the upper graph in Fig. 2. On an intermediate time scale the exact expression approaches the asymptotic linear behavior. From this figure it is clear that interactions between different path segments can be neglected if the intervals are separated by a time of $\sim 1/2\omega_c$. Finally, we examine the form of the imaginary part Q'' for large ω_c. After a time $t\sim 1/10\omega_c$ the function is constant. Figure 2(b) suggests to approximate the exact function by the step function given by Eq. (24).

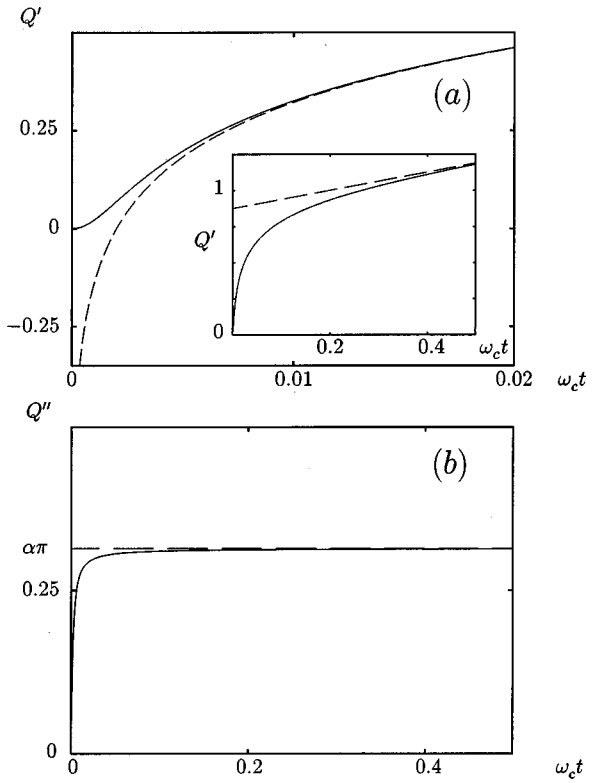

FIG. 2. In (a) the real part Q' of the twice-integrated kernel of the influence functional is shown. The full line depicts the exact result and the dashed line shows the high ω_c approximation. The function is shown for $t=0$ until $\omega_c t=0.02$. In the inset the full line depicts the exact result and the dashed line shows the linearized approximation. The function is shown for $t=0$ until $\omega_c t=0.5$. In (b) the imaginary part Q'' of the twice integrated kernel of the influence functional is shown. The full line depicts the exact result and the dashed line shows the step function for high ω_c. The function is shown for $t=0$ until $\omega_c t=0.5$. The dimensionless coupling strength α is 0.1 and the inverse temperature β is $1/\Delta$.

IV. THE INTERACTING-BLIP CHAIN APPROXIMATION

Recently, a formulation of the dynamics of driven dissipative two-state systems in terms of integral equations was introduced [13,24]. Starting from this formulation of the dynamical problem, more and more sophisticated approximations in the influence functional can be defined by systematically taking into account more and more interactions between different path segments in the influence functionals, which in turn give rise to increasingly more elaborate systems of integral equations. As linked clusters are generated by this approach, it has been named IBCA. Practical implementations, however, are setting limits on the range of the interactions included. The form of the influence functional given by Eq. (16) makes a decisive difference apparent between the dynamics of a two-state system and a multistate system. Imagine a two-state system evolving in time undergoing transitions between different states of the density matrix at times t_k starting out of a diagonal state. If the system leaves the diagonal of the density matrix, there are only two off-diagonal states it can occupy. After the succeeding transition the system is enforced to return to the diagonal. Such an excursion is called a *blip* whereas an intermediate segment of a path is called *sojourn* [26]. Each path is thus a succession of diagonal and off-diagonal segments; at any time t_k the system hops, it jumps from the diagonal to the off-diagonal or vice versa. In multistate systems the situation is somewhat different. If the system leaves the diagonal at the time $t=t_0$, it can undergo any number of transitions within the off-diagonal states until it returns to the diagonal. These excursions are now called *clusters* [28]. Within such a cluster, any interval has interactions via the real part of the influence functional with its neighbor without a sojourn in between.

In the sequel we approximate the influence functional by

neglecting all interactions with $r-s>1$ in Eq. (16), yielding

$$\tilde{\Phi}_{\mathrm{IBCA}}[\eta,\xi]=\sum_{r=0}^{N-1}(\xi_r^2\Lambda_{r,r}-i\xi_r\eta_r X_{r,r}) + \sum_{r=1}^{N-1}(\xi_r\Lambda_{r,r-1}\xi_{r-1}-i\xi_r X_{r,r-1}\eta_{r-1}). \tag{30}$$

If we introduce the quantities $\hat{\rho}_{\eta,\xi}(t,\tau)$ describing all paths that hopped into the state $\{\eta,\xi\}$ at time $t-\tau$ and remained there until the final time t, we can express the dynamics of the reduced density matrix in terms of coupled integral equations for the $\hat{\rho}_{\eta,\xi}(t,\tau)$.

The initial conditions are given by

$$\hat{\rho}_{\eta,\xi}(0,0)=\delta_{\eta,\eta_{\mathrm{init}}}\delta_{\xi,0}, \tag{31}$$

for a system that starts out of the diagonal state with the quasiclassical coordinate η_{init}. The dynamical equations corresponding to the influence function (30) are then given by

$$\hat{\rho}_{\eta,\xi}(t,\tau)=\int_0^{t-\tau}d\tau' \sum_{\eta'=\eta\pm1,\xi'=\xi\pm1} K_{\eta,\xi}^{\eta',\xi'}(\tau,\tau') \times\hat{\rho}_{\eta',\xi'}(t-\tau,t-\tau-\tau'), \tag{32}$$

where the $K_{\eta,\xi}^{\eta',\xi'}(\tau,\tau')$ are the kernels depending on the lengths of the intervals τ and τ'. The kernels describe the interaction between the actual and the proceeding interval. They are given by

$$K_{\eta_r,\xi_r}^{\eta_{r-1},\xi_{r-1}}(\tau_r,\tau_{r-1}) =-\mathrm{sgn}[(\xi_r-\xi_{r-1})(\eta_r-\eta_{r-1})]\frac{i\Delta}{2} \times\exp(-i\varepsilon_{\eta_r,\xi_r}\tau_r)\exp(\xi_r^2\Lambda_{r,r}-i\xi_r\eta_r X_{r,r}) \times\exp(\xi_r\Lambda_{r,r-1}\xi_{r-1}-i\xi_r X_{r,r-1}\eta_{r-1}). \tag{33}$$

The elements of the reduced density matrix are finally obtained by

$$\tilde{\rho}_{\eta,\xi}(t)=\delta_{\eta,\eta_{\mathrm{init}}}\delta_{\xi,0}+\int_0^t d\tau'\,\hat{\rho}_{\eta,\xi}(t,\tau'). \tag{34}$$

The first term in Eg. (34) takes into account the path that does not undergo any transition. By keeping trace of more and more interval lengths, the IBCA equations can be extended to a formally exact description of the dynamics. However, the higher-order equations are numerically untractable because of the algebraic growth of the required memory.

The simplest approximation to the influence functional yielding integral equations consists in taking into account the local interactions only. We then have

$$\tilde{\Phi}_{\mathrm{local}}[\eta,\xi]=\sum_{r=0}^{N-1}(\xi_r^2\Lambda_{r,r}-i\xi_r\eta_r X_{r,r}). \tag{35}$$

The kernels that correspond to the local interaction approximation of the influence functional (35) are given by

$$K_{\eta_r,\xi_r}^{\eta_{r-1},\xi_{r-1}}(\tau_r)=-\mathrm{sgn}[(\xi_r-\xi_{r-1})(\eta_r-\eta_{r-1})]\frac{i\Delta}{2} \times\exp(-i\varepsilon_{\eta_r,\xi_r}\tau_r)\exp(\xi_r^2\Lambda_{r,r}-i\xi_r\eta_r X_{r,r}). \tag{36}$$

The dynamical integral equations corresponding to the kernels (36) are then drastically simplified. They are given by

$$\hat{\rho}_{\eta,\xi}(t)=\int_0^t d\tau \sum_{\eta'=\eta\pm1,\xi'=\xi\pm1} K_{\eta,\xi}^{\eta',\xi'}(\tau)\hat{\rho}_{\eta',\xi'}(t-\tau). \tag{37}$$

Equations (37) are, however, already more general than the golden rule equations, because there is no restriction to the possible transitions between different diagonal states of the reduced density matrix invoked here. The approximation consists in treating the interactions of the influence functional only locally but still non-Markovian.

V. RESULTS

We study the dynamics of dissipative multistate systems with a moderate system-bath coupling $\alpha=0.1$ and Ohmic dissipation with a high cutoff frequency of $\omega_c=500/\Delta$, a value which is rather high so that the system will behave strictly Ohmic. In Sec. II, the formally exact solution of the problem was given. Despite recent progress in analytical as well as numerical approaches, a treatment of the dynamics avoiding any approximation is out of reach, if one wishes to perform simulations for intermediate to long propagation times. We discuss three different lines of approximation schemes.

(i) The exact influence functional given by Eq. (16) may be truncated. If only next-neighbor interactions are taken into account, the influence functional Eq. (30) is obtained. In principle, by cutting off the interactions after the mth-order next-neighbor interactions, a sequence of more and more sophisticated approximations can be defined, which in turn are more and more tedious to be evaluated.

(ii) The exact, twice-integrated kernel $Q(\tau)$ of the influence functional, Eq. (23), can be replaced by Eq. (24) in the scaling limit. In the resulting influence functional $\tilde{\Phi}_{\mathrm{FV}}^{\mathrm{Ohmic}}[\eta,\xi]$, Eq. (27), the time-nonlocal interactions only appear in the real part. In the weak coupling and high temperature regime, $Q(\tau)$ can be replaced by a linearized function given by Eq. (28). In the corresponding influence functional $\tilde{\Phi}_{\mathrm{FV}}^{\mathrm{lin}}[\eta,\xi]$, Eq. (29), only local interactions survive.

(iii) In principle, the system can evolve in time along any possible path in the reduced density matrix. Excursions away from the diagonal of the reduced density matrix act as a Gaussian filter in the configuration space [20]. Therefore, it is often possible to truncate the excursions away from the diagonal by some maximum value $\xi_{\max}$, i.e., $|\xi(\tau)|\leqslant\xi_{\max}$

olds for all times $0<\tau<t$. Setting $\xi_{\max}=1$ corresponds to the so-called sequential exchange mechanism.

The aim of this paper is to determine the range of validity of the different approximations in dependence of the temperature and the initial preparation. In principle, any combination of different approximations for $Q(\tau)$, the influence functional, and the exchange mechanism can be combined. However, if $Q(\tau)$ is linearized, all interblip correlations vanish. This illustrates that a linear $Q(\tau)$ is equivalent to a Markov approximation [2,24]. Generally speaking, the strength of the interblip correlations in the influence functional does not depend on the linear part of $Q(\tau)$ [see Eq. (19)]. The familiar golden-rule approximation consists in setting $\xi_{\max}=1$, and using the influence functional $\tilde{\Phi}_{\mathrm{IBCA}}[\eta,\xi]$, where $X_{r,r-1}$ is replaced by $\tilde{X}_{r,r-1}=-Q''(\tau_r)$. Within the golden rule $\xi_r\xi_{r-1}=0$ holds for all r.

Unfortunately, it is impossible to include all interactions exactly in numerical simulations if one does not use stochastic integration techniques [20] or alternative sophisticated approximation schemes [21,15]. The approximate influence function given by Eq. (30) underlying the dynamical integral Eq. (32) only takes into account next-neighbor interactions. A high cutoff frequency and moderate temperatures render the influence functional (30) a reliable approximation, because the interactions between separated path segments vanish if $Q(\tau)$ is linear, and we have seen that the deviations of $Q(\tau)$ from linearity are relevant at short times only (see Fig. 2). The dynamical Eq. (32) intrinsically generates a cluster expansion. A cluster is a sequence of propagation intervals, that leaves the diagonal of the reduced density matrix at a time t_{init} and returns to the diagonal at a later time t_{final}. During a cluster the system may undergo any number of transitions between off-diagonal states but never comes back to nor crosses the diagonal. To take into account interactions between clusters, second next-neighbor interactions must be considered.

The calculations presented here are for dissipative 5-state systems, and we consider two different initial conditions: a symmetric state and an edge state. Interestingly enough, the accuracy of employed approximations depends on the initial state. We present results for the time evolution of the diagonal elements of the reduced density matrix $\langle\tilde{\rho}_{j,0}(t)\rangle_\beta$, which we denote by $P_j(t)$ henceforth. In Sec. V A we study unbiased systems. Biased systems are investigated in Sec. V B.

A. Unbiased systems

First we focus our attention on systems with zero static bias ($e_1=\cdots=e_5=0$). In Fig. 3(a), the survival probabilities $P_j(t)$ are shown for the temperature $\beta=0.1/\Delta$. The system is initially prepared in the state $|\varphi_3\rangle$. Because of the symmetry of the system, $P_1(t)$ and $P_5(t)$ as well as $P_2(t)$ and $P_4(t)$ coincide. The graphs of $P_4(t)$ and $P_5(t)$ are, therefore, omitted in Fig. 3. The dynamics is described very accurately by the Markov approximation corresponding to the interaction given by Eq. (28), and it is almost completely dominated by the sequential exchange processes. The contributions of paths, which travel further away from the diagonal of the reduced density matrix, are negligible. The differences

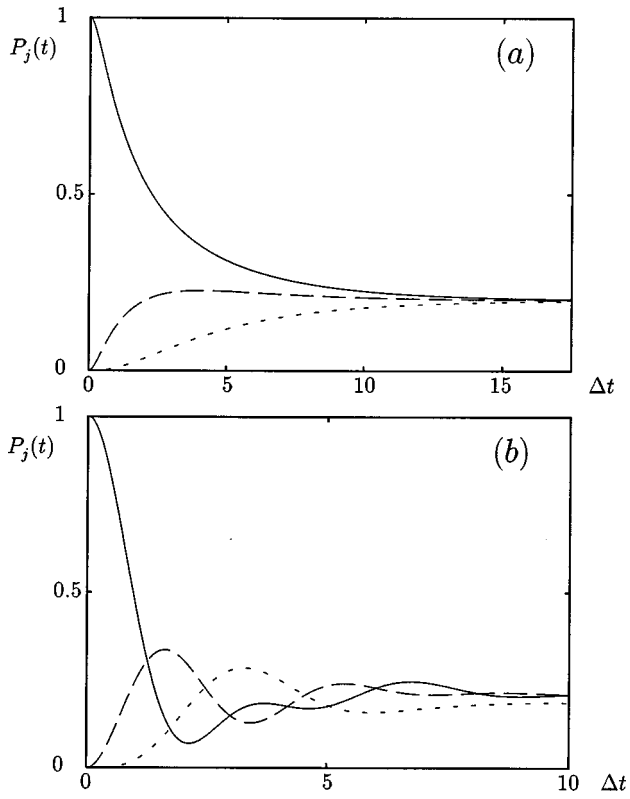

FIG. 3. Survival probabilities for the temperatures $\beta=0.1/\Delta$ (a) and $\beta=1/\Delta$ (b). The system is initially prepared in the state $|\varphi_3\rangle$. The dimensionless coupling strength α is 0.1 [full lines $P_3(t)$, long-dashed lines $P_2(t)=P_4(t)$, short-dashed lines $P_1(t)=P_5(t)$].

are almost invisible on the scale of Fig. 3(a). The situation changes considerably if we reduce temperature by a factor of ten. In Fig. 3(b), the survival probabilities $P_1(t)$, $P_2(t)$, and $P_3(t)$ are plotted for $\beta=1/\Delta$. In this temperature regime the Markov approximation breaks down. Replacing the exact expression (23) by the corresponding Ohmic form (24), however, results in negligible differences in the results. The divergence of the expression $Q'(t)$ that occurs if t tends to zero, does not spoil numerical simulations on a grid in time, if the latter is coarse enough. The convergence of the results has been checked empirically. In this temperature regime the dynamics is no longer controlled by the sequential exchange mechanism. Processes with $\xi_{\max}=2$ must be taken into account. In Fig. 4, the full line corresponds to $\xi_{\max}=2$, and the dashed line to $\xi_{\max}=1$. Clusters which travel further away from the diagonal can be neglected on the scale shown in Fig. 4.

So far we considered the dynamics of systems prepared in the state $|\varphi_3\rangle$. Starting out from this state, the system can move in both directions along the discretized system coordinate with equal probabilities. Now we study the dynamics of systems, which start out from the edge state $|\varphi_1\rangle$. Figure 5(a) shows the population probabilities $P_j(t)$ for a temperature $\beta=0.1/\Delta$. The relaxation towards the equilibrium value of the population probabilities $P_j(t)$ is much slower than for a symmetric initial preparation. Again, for this temperature, the dynamics is exactly reproduced by the Markov approximation, and it is determined by the sequential exchange mechanism. This also holds true for the temperature $\beta=1/\Delta$. The results are depicted in Fig. 5(b). The only differ-

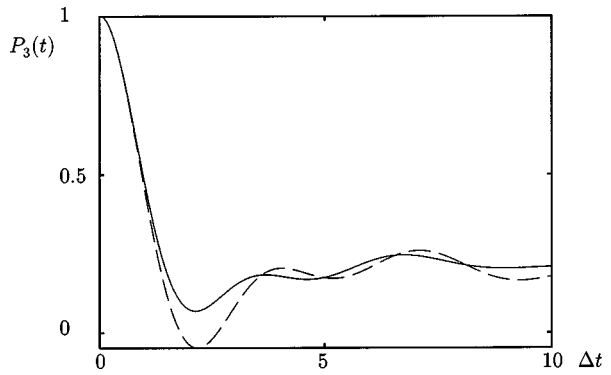

FIG. 4. Survival probability $P_3(t)$ for a temperature $\beta=1/\Delta$. The full curve depicts the result for $\xi_{\max}=2$. The dashed line represents the sequential exchange result. The dimensionless coupling strength α is 0.1.

ence in the dynamics depicted in Figs. 3 and 5 is a different initial value. For a symmetric initial state the Markov approximation fails and second-order superexchange transitions must be taken into account. On the contrary, if the system starts out of an edge state, the accuracy of the Markov approximation is excellent and the dynamics is totally controlled by sequential transitions. From this we conclude that the validity of different approximations is not only depending on the model parameters such as temperature or coupling strength, but is also highly sensitive to the initial state.

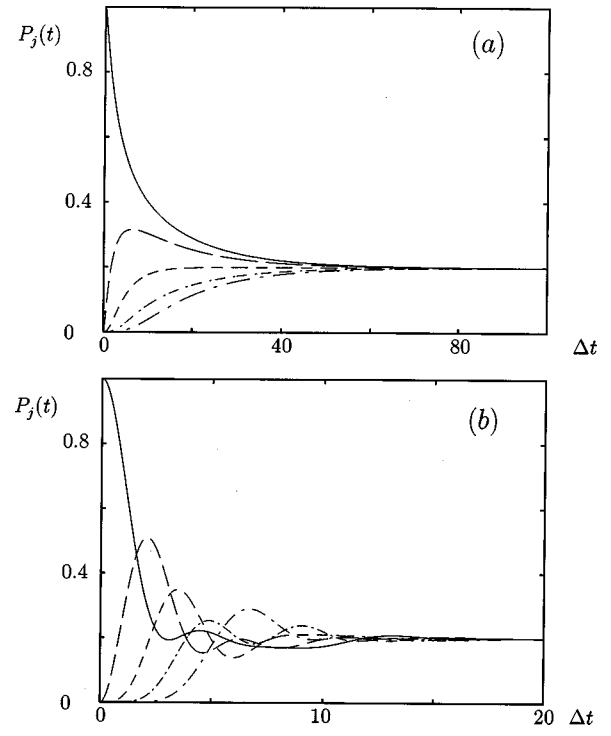

FIG. 5. Survival probabilities $P_j(t)$ for the temperatures $\beta=0.1/\Delta$ (a) and $\beta=1/\Delta$ (b). The system is prepared in the state $|\varphi_1\rangle$. The tunneling dynamics is exactly reproduced by the Markov approximation. The dimensionless coupling strength α is 0.1 [full lines $P_1(t)$, long-dashed lines $P_2(t)$, short-dashed lines $P_3(t)$, short dash-dotted lines $P_4(t)$, and long dash-dotted lines $P_5(t)$].

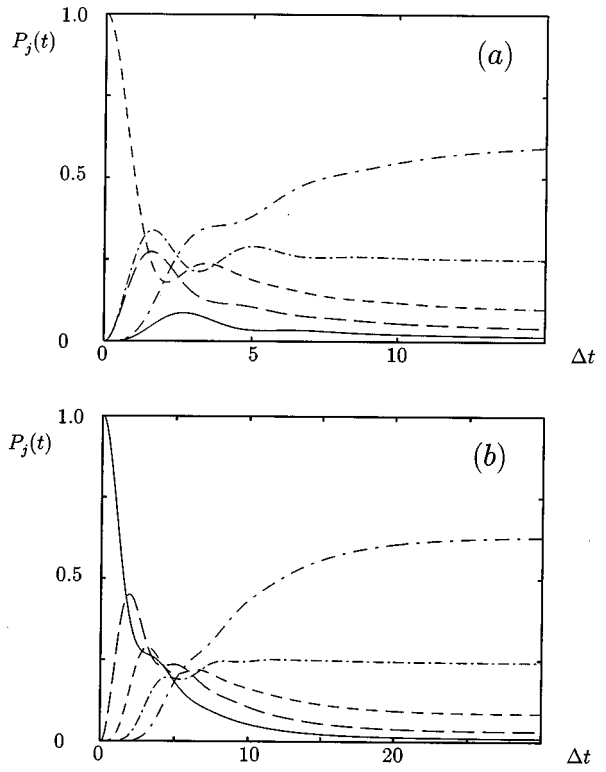

FIG. 6. Survival probabilities $P_j(t)$ for the temperature $\beta=1/\Delta$ and a bias $e_j=(3-j)\Delta$. In the upper graph (a), the system is prepared in the state $|\varphi_3\rangle$ and in the bottom graph (b) the system is prepared in the edge state $|\varphi_1\rangle$. The dimensionless coupling strength α is 0.1 [full lines $P_1(t)$, long-dashed lines $P_2(t)$, short-dashed lines $P_3(t)$, short dash-dotted lines $P_4(t)$, and long dash-dotted lines $P_5(t)$].

B. Biased systems

We now study a biased system with $e_1=2\Delta$, $e_2=1\Delta$, $e_3=0$, $e_4=-1\Delta$, and $e_5=-2\Delta$ for a temperature of $\beta=1/\Delta$. The survival probabilities are shown in Figs. 6(a) and 6(b) for an initial preparation in the state $|\varphi_3\rangle$ and $|\varphi_1\rangle$, respectively. For the initial state $|\varphi_1\rangle$ the oscillations prevail almost twice as long.

In Fig. 7(a), $P_3(t)$ is shown for three different approximations for a symmetric initial value. The full line corresponds to the IBCA and the short-dashed line to the Markov approximation. The long-dashed line shows the calculation where only the local contributions of the influence functional were taken into account. This corresponds to setting $\Lambda_{j,k}=0$ for $k<j$. Here the coherent oscillations are overestimated remarkably by the Markov approximation. It is obvious from Fig. 7(a) that the next-neighbor interactions in the influence functional lead to qualitative corrections.

For a system with an initial state $|\varphi_1\rangle$, the time evolution of the population of this state is shown in Fig. 7(b). Here the dynamics is fairly well reproduced by the Markov approximation. For all simulations of the biased system second-order superexchange transitions ($x_{\max}=2$) must be taken into account.

This result makes clear that approximations must be carefully chosen. From Fig. 7(a) it is clear that for a system, which is initially prepared in the center state $|\varphi_3\rangle$, the next-neighbor interblip interactions are crucial, whereas Fig. 7(b)

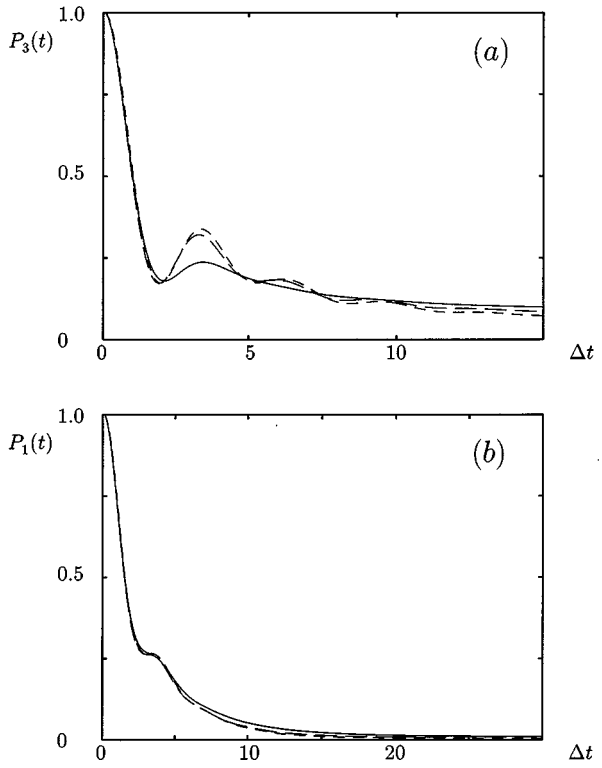

FIG. 7. (a) $P_3(t)$ for the same parameters as Fig. 6(a). (b) $P_1(t)$ for the same parameters as Fig. 6(b). The full lines correspond to the IBCA, the long-dashed lines correspond to the local interaction, and the short-dashed lines correspond to the Markov approximation.

shows that for the initial state $|\varphi_1\rangle$, even the Markov approximation is almost quantitative. Superexchange processes must, however, be taken into account.

VI. CONCLUSIONS AND OUTLOOK

The recently introduced description of the dynamics of driven dissipative two-state systems in terms of coupled integral equations, denoted IBCA, has been extended to multilevel systems. There is a qualitative difference due to the richer combinatorics of a multilevel system. In a two-state system the excursions away from the diagonal of the reduced density matrix are of second order in the intersite coupling matrix element. Consequently, every path is a succession of diagonal and off-diagonal intervals. On the contrary, in the multilevel system, there are clusters, excursions away from the diagonal, of any even order in the coupling matrix element, and, therefore, next-neighbor intervals exhibit interactions in the real as well as the imaginary part of the time-nonlocal influence functional. In principle, the system can propagate along any path in the reduced density matrix. The real part of the influence functional, however, acts as a Gaussian filter in the quantum fluctuations. If the temperature and/or coupling is strong, clusters, which travel far away from the diagonal, are effectively suppressed and as a consequence the exchange is dominated by sequential processes or processes that have a maximum quantum fluctuation $\xi_{\max}$. Interestingly, the validity of the Markov or local interaction approximation depends crucially on the initial state. Moreover, the same is true for the predominating exchange mechanism. If the system starts out from the central state, long-range interactions and thus higher-order exchange mechanisms are more important than for the dynamics of systems that start out of an edge state.

As an illustrative example, a 5-state system with a moderate coupling and an Ohmic spectral density with very high cutoff frequency was studied for two different temperatures. The accuracy of the strict Ohmic and the Markovian approximation for the interactions entering the influence functional was investigated. For a cutoff frequency of $\omega_c = 500\Delta$ the simplified version of the interactions given by Eq. (24) is an adequate approximation. The phase originating from the imaginary part of the influence functional gives rise to next-neighbor interactions only. The real part contains interactions between any segments of a path. In the Markov approximation the interactions are local and in the case of a high cutoff frequency they are rapidly decaying. In such a case the first-order IBCA equations give an excellent description of the dynamics. The extension to driven systems is the contents of current research.

ACKNOWLEDGMENTS

This work has been supported by the Deutsche Forschungsgemeinschaft (DFG) through the Sonderforschungsbereich 382. The author would like to thank M. Grifoni, G. Lang, J. Rollbühler, and Professor U. Weiss for stimulating discussions.

[1] C.W. Gardiner, *Handbook of Stochastic Methods* (Springer, Berlin, 1985).
[2] U. Weiss, *Quantum Dissipative Systems* (World Scientific, Singapore, 1993); *Quantum Dissipative Systems*, 2nd ed. (World Scientific, Singapore, 1999).
[3] R.P. Feynman, Rev. Mod. Phys. **20**, 367 (1948).
[4] R.P. Feynman and A.R. Hibbs, *Quantum Mechanics and Path Integrals* (McGraw-Hill, New York, 1965).
[5] L.S. Schulman, *Techniques and Applications of Path Integrals* (McGraw-Hill, New York, 1981).
[6] R.P. Feynman and F.L. Vernon, Ann. Phys. (N.Y.) **24**, 118 (1963).
[7] M.P.A. Fisher and W. Zwerger, Phys. Rev. B **32**, 6190 (1985). W. Zwerger, *ibid.* **35**, 4737 (1987).
[8] G. Schön and A.D. Zaikin, Phys. Rep. **198**, 237 (1990).
[9] C.L. Kane and M.P.A. Fisher, Phys. Rev. Lett. **68**, 1220 (1992).
[10] X.G. Wen, Phys. Rev. B **41**, 12 838 (1990); **43**, 11 025 (1991); **44**, 5708 (1991).
[11] U. Weiss, M. Sassetti, T. Negele, and M. Wollensak, Z. Phys. B **84**, 471 (1991).
[12] G.M. Lucke, C.M Mak, R. Egger, J. Ankerhold, J. Stockburger, and H. Grabert, J. Chem. Phys. **107**, 8397 (1997).

[13] M. Winterstetter and U. Weiss, Chem. Phys. **217**, 155 (1997); M. Grifoni, M. Winterstetter, and U. Weiss, Phys. Rev. E **56**, 334 (1997).
[14] M.F. Trotter, Proc. Am. Math. Soc. **10**, 545 (1959).
[15] M. Winterstetter and U. Weiss, Chem. Phys. **209**, 455 (1996); M. Winterstetter and W. Domcke, Chem. Phys. Lett. **236**, 455 (1995).
[16] R. Egger and C.H. Mak, Phys. Rev. B **50**, 15 210 (1994); J. Phys. Chem. **98**, 9903 (1994).
[17] D. Makarov and N. Makri, J. Chem. Phys. **102**, 4611 (1995).
[18] R.D. Coalson, Phys. Rev. B **39**, 12 052 (1989); J. Chem. Phys. **94**, 1108 (1991); R.D. Coalson, D.G. Evans, and A. Nitzan, *ibid.* **101**, 436 (1994).
[19] C.H. Mak and D. Chandler, Phys. Rev. A **44**, 2352 (1991).
[20] C.H. Mak and R. Egger, Adv. Chem. Phys. **XCIII**, 39 (1996).
[21] N. Makri, J. Math. Phys. **36**, 2430 (1995).
[22] A.G. Redfield, Adv. Magn. Reson. **1**, 1 (1965).
[23] A. Benderskii, D.E. Makarov, and C.A. Wight, Adv. Chem. Phys. **88**, 1 (1994).
[24] M. Grifoni, M. Winterstetter, and U. Weiss, Phys. Rev. E **56**, 334 (1997).
[25] O. Kühn, V. May, and M. Schreiber, J. Chem. Phys. **101**, 10 404 (1994).
[26] A.J. Leggett, S. Chakravarty, A.T. Dorsey, M.P.A. Fisher, A. Garg, and W. Zwerger, Rev. Mod. Phys. **59**, 1 (1987).
[27] M. Sassetti and U. Weiss, Phys. Rev. A **41**, 5383 (1990).
[28] R. Egger, C.H. Mak, and U. Weiss, Phys. Rev. E **50**, R655 (1994).
[29] M. Grifoni, M. Sassetti, and U. Weiss, Phys. Rev. E **53**, R2033 (1996).
[30] R. Egger and U. Weiss, Z. Phys. B **89**, 97 (1992).